Modeling power law absorption and dispersion for acoustic propagation using the fractional Laplacian

Bradley E. Treeby[a] and B. T. Cox
Department of Medical Physics and Bioengineering, University College London, Gower Street, London WC1E 6BT, United Kingdom

(Received 24 November 2009; revised 26 February 2010; accepted 10 March 2010)

The efficient simulation of wave propagation through lossy media in which the absorption follows a frequency power law has many important applications in biomedical ultrasonics. Previous wave equations which use time-domain fractional operators require the storage of the complete pressure field at previous time steps (such operators are convolution based). This makes them unsuitable for many three-dimensional problems of interest. Here, a wave equation that utilizes two lossy derivative operators based on the fractional Laplacian is derived. These operators account separately for the required power law absorption and dispersion and can be efficiently incorporated into Fourier based pseudospectral and *k*-space methods without the increase in memory required by their time-domain fractional counterparts. A framework for encoding the developed wave equation using three coupled first-order constitutive equations is discussed, and the model is demonstrated through several one-, two-, and three-dimensional simulations. © *2010 Acoustical Society of America.*
[DOI: 10.1121/1.3377056]

PACS number(s): 43.20.Bi, 43.20.Hq, 43.35.Bf, 43.35.Wa [TDM] Pages: 2741–2748

I. INTRODUCTION

The derivation of wave equations to model acoustic absorption and dispersion in biological tissue has continued to be a subject of research interest over the last decade. Although many approaches have been suggested, each represents a compromise between correctly modeling experimentally observed absorption and dispersion, meeting causality requirements, and allowing efficient numerical computation. The latter is often overlooked to allow satisfying the former, but computational efficiency is particularly important for modeling three-dimensional (3D) wave propagation in large and potentially heterogeneous domains. For periodic *k*-space and pseudospectral time-domain methods in which spatial derivatives are computed globally using the Fourier transform (this reduces the number of grid points required per wavelength compared to conventional finite difference methods),[1,2] an efficient approach for including arbitrary power law absorption has not yet been proposed. It is this deficiency that is the subject of interest here.

The motivation for deriving a lossy wave equation for tissue ultrasonics stems from the strong dependence of the amplitude, spectrum, and shape of propagating ultrasound pulses on the absorption characteristics of tissue media. For diagnostic imaging, these effects limit the depth at which tissues can be imaged and cause the pulse shape to be path-length dependent.[3] The simulation of tissue-realistic ultrasound propagation assists in the development of image reconstruction and speckle reduction techniques, and in the extraction of pathological features from analog radio-frequency data. For therapeutic technologies such as high intensity focused ultrasound, simulation plays an important role in sensor design, treatment planning, and condition monitoring.[4] For photoacoustic tomography (an imaging modality based on the thermoelastic generation of ultrasound through pulsed laser light),[5] the resolution of reconstructed images is dependent on the available frequency content, which in turn is dependent on the medium absorption. Here, simulations form an integral part of both image reconstruction,[6] and the extraction of quantitative information.[7] The success of such simulations is inherently linked to the availability of techniques to accurately and efficiently model ultrasound wave propagation with tissue-realistic acoustic parameters.

Here, a lossy equation of state for modeling power law absorption and dispersion that can be efficiently incorporated into Fourier based pseudospectral and *k*-space methods is derived. First, the available approaches for modeling power law absorption and dispersion are reviewed. A lossy wave equation based on the fractional Laplacian that accounts for the power law absorption and dispersion evident in biological tissue is then developed. Next, a flexible framework for including absorption into pseudospectral and *k*-space models based on first-order coupled equations is introduced. Finally, using this approach, the efficacy of the model is demonstrated through several numerical simulations.

II. MODELING POWER LAW ABSORPTION AND DISPERSION

A. Lossy wave equations using fractional derivative operators

It is well known that over diagnostic ultrasound frequencies, acoustic absorption in biological tissue exhibits a power law frequency dependence of the form

[a]Author to whom correspondence should be addressed. Electronic mail: btreeby@mpb.ucl.ac.uk

TABLE I. Lossy derivative operators for Eq. (2).

	Damped	Blackstock	Szabo	Stokes	Chen and Holm	Caputo/ Wismer
Π	$\frac{\partial}{\partial t}$	$\frac{\partial^3}{\partial t^3}$	$\frac{\partial^{y+1}}{\partial t^{y+1}}$	$\frac{\partial}{\partial t}\nabla^2$	$\frac{\partial}{\partial t}(-\nabla^2)^{y/2}$	$\frac{\partial^{y-1}}{\partial t^{y-1}}\nabla^2$
$\alpha\propto$	ω^0	ω^2	ω^y	ω^2	ω^y	ω^y

$$\alpha = \alpha_0 \omega^y, \tag{1}$$

where α_0 is the absorption coefficient in $\mathrm{Np(rad/s)}^{-y}\,\mathrm{m}^{-1}$, ω is the angular frequency in rad/s, and the power law exponent y is typically in the range $1 \le y \le 1.5$.[3] However, classical lossy wave equations predict an absorption that is either frequency independent, or proportional to frequency squared.[8] Szabo made the observation that for a lossy wave equation of the form

$$\frac{1}{c_0^2}\frac{\partial^2 p}{\partial t^2} = \nabla^2 p + \tau \Pi p \tag{2}$$

(here p is the acoustic pressure, c_0 is the thermodynamic speed of sound, Π is a general derivative operator, and τ is a proportionality coefficient), the power law exponent y of the resulting frequency dependent absorption was 1 less than the order of the derivative operator Π.[9] Based on this observation, Szabo then derived a causal convolution operator that accounted for power law absorption with a noninteger frequency dependence. This operator was later rewritten as a fractional derivative by both Chen and Holm[10] and Liebler *et al.*,[11] and then derived more formally by Kelly *et al.*[12] A similar operator (although written as a convolution) was also used by Buckingham.[13] It is evident from this form of Szabo's wave equation that the fractional operator interpolates between the damped (or telegraphers) and Blackstock wave equations on which it was originally based (see Table I).

The same analogy between the order of the derivative operator Π and the observed power law exponent y was used by Chen and Holm[14] and Wismer[15] to derive fractional derivative operators based on Stokes' wave equation. (The operator used by Wismer also appears nearly four decades earlier in Caputo's seminal paper on fractional derivatives.[16]) While Caputo/Wismer used a fractional time domain operator, Chen and Holm utilized the idea of a fractional Laplacian. Ochmann and Makarov also used the fractional derivative to account for power law absorption in Burgers' equation.[17,18] A summary of the relevant derivative operators and the resulting absorption frequency dependence is given in Table I.

B. Fractional operators and memory

The function of the fractional lossy derivative operators can be more clearly understood using the idea of linear filters. Employing a generalized function approach, Caputo's fractional derivative may be written in the form[19]

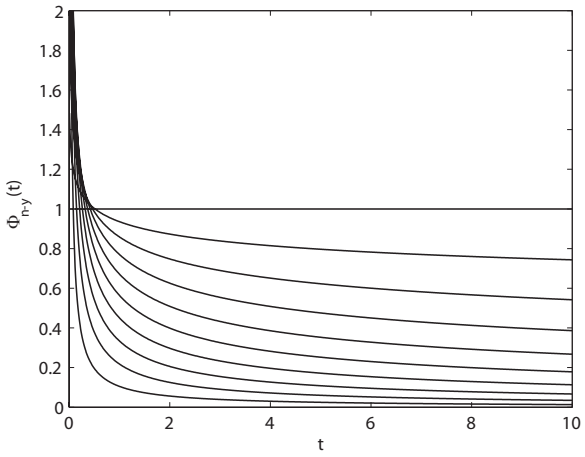

FIG. 1. Decay of the convolution function $\Phi_{n-y}(t)$ used in the generalized function form of the fractional derivative. The ten curves illustrate values of $(n-y)$ from 1 (upper curve) to 0.1 (lower curve) in increments of 0.1.

$$\frac{\partial^y f(t)}{\partial t^y} = \frac{\partial^n f(t)}{\partial t^n} * \Phi_{n-y}(t). \tag{3}$$

Here y is a positive real number, n is an integer defined by $n-1 \le y < n$, $*$ is the convolution operator, and the function $\Phi_{n-y}(t)$ is given by

$$\Phi_{n-y}(t) = \begin{cases} \dfrac{t^{n-y-1}}{\Gamma(n-y)} & \text{for} \quad t > 0 \\ 0 & \text{for} \quad t \le 0 \end{cases} \tag{4}$$

(the Riemann–Liouville definition of the fractional derivative can also be written in a similar form but the derivative is taken after the convolution). The behavior of the fractional derivative can then be divided into three categories depending on the characteristics of the function $\Phi_{n-y}(t)$ (see Fig. 1). First, for $(n-y)=\epsilon^+$ (where ϵ^+ is the positive infinitesimal), $\Phi_{\epsilon^+}(t)$ approaches a one-sided delta function and thus the fractional derivative does not have any memory.[20] In this case the output of the convolution is simply equal to value of the input function $\partial^n f(t)/\partial t^n$ at the current time t. Second, for $(n-y)=1$, $\Phi_1(t)$ becomes a Heaviside step function and thus the fractional derivative has complete memory in which all previous states of the input function contribute equally to the output. In this case the output is given by the conventional single integral of the input function $\partial^n f(t)/\partial t^n$. Finally, for $0<(n-y)<1$, the fractional derivative has partial memory in which the current state of the input function is given the maximum weighting and the weighting of the previous states decays according to $\Phi_{n-y}(t)$ (see Fig. 1). Without invoking other analytical or numerical forms of the fractional derivative, it is clear that the numerical computation of fractional operators of this form will require knowledge, viz., storage, of the input's time history.

The form of the fractional derivative given in Eq. (3) can be used to qualitatively assess the memory requirements for particular values of the power law exponent (irrespective of the actual implementation of the operators). Returning to Szabo and Caputo/Wismer's fractional derivative operators given in Table I, for a fractional power law exponent on the interval $1<y<2$, the convolution function will take the

form $\Phi_{2-y}(t)$. If y is close to 2, this function will decay rapidly and consequently the fractional derivative can be approximated using only a small number of previous time steps (this is known as the "short memory principle").[19] Conversely, if y is close to 1, $\Phi_{2-y}(t)$ will decay slowly (recall $\Phi_1(t)$ is the step function) and thus the fractional derivative will be dependent on a large number of previous time steps. This effect was noted numerically by Wismer who simulated wave propagation in an axisymmetric 3D domain using the finite element method.[15] Here the fractional derivative was computed for $y=1.4$ via Grünwald–Letnikov's formula using a history of 10, 15, and 20 time steps, and even the latter was insufficient to reach convergence. To overcome this memory burden, Liebler *et al.*[11] proposed a recursive algorithm in which the nonlocal part of the fractional derivative was approximated by a sum of decaying exponentials. However, this approach is somewhat heuristic and requires an *a priori* parameter optimization for each value of y. Additionally, a time history of three to four steps and up to ten auxiliary fields are still required.

In the context of deriving an efficient method for modeling power law absorption (for pseudospectral and k-space methods, in particular), the derivative operator suggested by Chen and Holm[14] based on the fractional Laplacian appears to be the most promising. In this case, no additional storage is required as the value of the propagating wave at other positions (rather than times) is already known. For Fourier based pseudospectral methods, the implementation of a fractional Laplacian does not pose any particular numerical difficulties as spatial derivatives are already computed in the spatial frequency domain. Indeed, for both integer and fractional powers of the negative Laplacian, the Fourier transform is simply given by[14]

$$\mathcal{F}_r\{(-\nabla^2)^n f(r)\} = k^{2n}\mathcal{F}_r\{f(r)\}, \tag{5}$$

where k is the magnitude of the spatial wavenumber (this implicitly assumes a fractional derivative of the form ${}_{-\infty}D_t^y$).[19] However, although the operator proposed by Chen and Holm appears to correctly model power law absorption, it has been suggested that it does not exhibit the correct dispersive sound speed.[21] This is shown in Sec. III A of the current work, and an alternative equation, also based on the fractional Laplacian, is proposed.

C. Other approaches to modeling power law absorption

Before continuing, it is useful to note there are several other methods for modeling lossy wave propagation as an alternative to wave equations in the form of Eq. (2).[3,22–25] However, most of these become computationally formidable for 3D problems of practical interest. The most apposite alternative is the model proposed by Nachman *et al.*[22] which utilizes a spectrum of relaxation times. This approach can be incorporated into both finite difference[26] and k-space[27] propagation models, and recently has been used to model attenuation and dispersion in media with $y=1$.[28,29] However, to model the power law absorption observed in biological tissue, a distribution of relaxation parameters must first be fitted. This becomes cumbersome for simulating broadband pulse propagation for arbitrary power law parameters, and there is no evidence that the derived relaxation times have any physical meaning. An explicit k-space model for $y=1$ has also previously been derived for modeling initial value problems in photoacoustic tomography.[30] However, while this facilitates efficient numerical computation, the utilized governing wave equation is nondispersive.

III. DEVELOPMENT OF A LOSSY WAVE EQUATION

A. Analysis of the fractional Laplacian wave equation

The lossy wave equation based on the fractional Laplacian proposed by Chen and Holm[14] is given by

$$\frac{1}{c_0^2}\frac{\partial^2 p}{\partial t^2} = \nabla^2 p + \tau\frac{\partial}{\partial t}(-\nabla^2)^{y/2} p, \tag{6}$$

where the proportionality coefficient τ is

$$\tau = -2\alpha_0 c_0^{y-1}. \tag{7}$$

Substituting the plane wave solution $p \propto e^{i(\tilde{k}x-\omega t)}$ where $\tilde{k}$ is the complex wavenumber (any general field can be written as a sum of plane waves) yields the following dispersion relation

$$\tilde{k}^2 = \frac{\omega^2}{c_0^2} + \tau(-i\omega)\tilde{k}^y \tag{8}$$

(here the fractional Laplacian of the exponential function is given analogous to the relationship implicitly used in Eq. (5)).[19] Splitting the wavenumber into real and imaginary parts where $\tilde{k}=k_r+ik_i$ then gives

$$k_r^2 + 2ik_rk_i - k_i^2 = \frac{\omega^2}{c_0^2} + \tau(-i\omega)(k_r+ik_i)^y. \tag{9}$$

Here $k_r=\omega/c_p$ encapsulates the propagating part of the wave (where c_p is the frequency dependent phase speed), and $k_i=\alpha$ encapsulates the absorption. Using the smallness approximation $k_i \ll k_r$ (which is valid for biologically relevant ultrasound absorption),[9] the final term can be expanded using the first two terms of a binomial series giving

$$k_r^2 + 2ik_rk_i - k_i^2 = \frac{\omega^2}{c_0^2} + \tau(-i\omega)k_r^y(1+iyk_i/k_r). \tag{10}$$

Collecting real and imaginary terms then yields

$$k_r^2 - k_i^2 - \omega^2/c_0^2 - \tau\omega y k_r^{y-1}k_i = 0 \quad \text{(real)},$$

$$2k_rk_i + \tau\omega k_r^y = 0 \quad \text{(imag)}. \tag{11}$$

The imaginary expression can be rearranged as

$$k_r^{y-1} = -\frac{2k_i}{\tau\omega}, \tag{12}$$

which allows the real part to be written in the form

$$k_r^2 = \frac{\omega^2}{c_0^2} + (1-2y)k_i^2. \tag{13}$$

It immediately follows that for $k_i \ll k_r$, $k_r \approx \omega/c_0$ and thus

$$c_p \approx c_0. \tag{14}$$

Equation (12) can then be written as

$$k_i \approx -\frac{\tau\omega^y}{2c_0^{y-1}} = \alpha_0\omega^y. \tag{15}$$

From Eqs. (14) and (15) it is evident that the wave equation proposed by Chen and Holm [given in Eq. (6)] exhibits the desired power law absorption but is nondispersive.

B. Deriving an alternative wave equation

A physical inconsistency in Chen and Holm's equation arises because the propagation of a sound wave through an absorbing medium is intrinsically linked with dispersion (a dependence of the phase speed on frequency). For power law absorption in the form of Eq. (1), the required dispersive phase speed c_p can be derived using the Kramers–Kronig relations. For $0<y<3$ and $y\neq 1$, this gives[31,32]

$$\frac{1}{c_p} = \frac{1}{c_{\omega_0}} + \alpha_0 \tan(\pi y/2)(\omega^{y-1} - \omega_0^{y-1}) \tag{16}$$

(an alternate expression is also available for $y=1$).[31] Here the dispersion is given as a variation from a reference sound speed c_{ω_0} at a particular frequency ω_0. A dispersion relation that satisfies both Eqs. (1) and (16) is given by[12]

$$\tilde{k} = \frac{\omega}{c_0} - \frac{\alpha_0(-i)^{y+1}\omega^y}{\cos(\pi y/2)}, \tag{17}$$

where the exact form of the encapsulated dispersion is

$$\frac{1}{c_p} = \frac{1}{c_0} + \alpha_0 \tan(\pi y/2)\omega^{y-1}. \tag{18}$$

Taking the square of this dispersion relation

$$\tilde{k}^2 = \frac{\omega^2}{c_0^2} - \frac{2\alpha_0(-i\omega)(-i)^y\omega^y}{c_0\cos(\pi y/2)} - \frac{\alpha_0^2(-i\omega)^{2y}}{\cos^2(\pi y/2)}, \tag{19}$$

neglecting second-order absorption terms (analogous to the smallness approximation $k_i \ll k_r$) and using the result $(-i)^y = \cos(\pi y/2) - i\sin(\pi y/2)$ then yields

$$\tilde{k}^2 = \frac{\omega^2}{c_0^2} + \frac{2i\alpha_0\omega^{y+1}}{c_0} + \frac{2\alpha_0\tan(\pi y/2)\omega^{y+1}}{c_0}. \tag{20}$$

This expression can be used to examine and derive derivative operators analogous to those given in Table I.

From the preceding analysis, it is evident that a wave equation that exhibits both absorption and dispersion must correspondingly yield both real and imaginary perturbations to the lossless dispersion relation $k^2 = \omega^2/c_0^2$. To first order, the real part corresponds to the encapsulated dispersion and the imaginary part the absorption. Again neglecting second-order absorption terms, the dispersion relation for Chen and Holm's lossy wave equation can be rewritten using Eqs. (14) and (15),

$$\tilde{k}^2 = \frac{\omega^2}{c_0^2} + \frac{2i\alpha_0\omega^{y+1}}{c_0}. \tag{21}$$

Comparing this with Eq. (20) highlights the absence of a perturbation to the real part of $\tilde{k}$. To correct for this deficiency, an additional derivative operator is required that yields this perturbation. To allow computational efficiency equivalent to Chen and Holm's original equation, the additional operator must also be dependent on the fractional Laplacian (rather than temporal fractional operators).

Starting with Stokes' lossy derivative operator (see Table I), removing the temporal derivative and adjusting the Laplacian exponent to give the correct power law dependence yields

$$\Pi = (-\nabla^2)^{(y+1)/2}. \tag{22}$$

Letting the corresponding proportionality coefficient be equal to η, this produces a dispersion relation of the form

$$\tilde{k}^2 = \frac{\omega^2}{c_0^2} + \eta\tilde{k}^{y+1}. \tag{23}$$

Expanding $\tilde{k}$ into real and imaginary parts under the smallness assumption $k_i \ll k_r$ and neglecting second-order absorption terms yields the result $\tilde{k} \approx k_r$ (i.e., the operator is nonabsorbing). Substituting $k_r = \omega/c_p$ then gives

$$\frac{1}{c_p^2} = \frac{1}{c_0^2} + \frac{\eta\omega^{y-1}}{c_p^{y+1}}. \tag{24}$$

Taking the square root and then expanding the term on the right hand side using the first two terms of a binomial series under the smallness approximation $\eta\omega^{y-1}c_0^2/c_p^{y+1} \ll 1$ (i.e., the amount of dispersion is small in relation to the thermodynamic sound speed c_0), this becomes

$$\frac{1}{c_p} = \frac{1}{c_0} + \frac{\eta c_0\omega^{y-1}}{2c_p^{y+1}}. \tag{25}$$

A first-order approximation for c_p can then be obtained by replacing c_p with c_0 on the right hand side which yields

$$\frac{1}{c_p} = \frac{1}{c_0} + \frac{\eta\omega^{y-1}}{2c_0^y}. \tag{26}$$

If the proportionality coefficient is given by

$$\eta = 2\alpha_0 c_0^y \tan(\pi y/2), \tag{27}$$

then Eq. (26) is identical to Eq. (18) as required. In contrast to the operator discussed in the previous section, Eq. (22) exhibits the desired power law dispersion but is nonabsorbing. A lossy wave equation that exhibits the correct power law absorption and dispersion can then be obtained by combining the two operators. This yields

$$\frac{1}{c_0^2}\frac{\partial^2 p}{\partial t^2} = \nabla^2 p + \left\{\tau\frac{\partial}{\partial t}(-\nabla^2)^{y/2} + \eta(-\nabla^2)^{(y+1)/2}\right\}p, \tag{28}$$

where the proportionality coefficients τ and η are given by Eqs. (7) and (27), respectively. Under the same smallness approximations used previously, the corresponding dispersion relation is given by Eq. (20). Note, this expression is

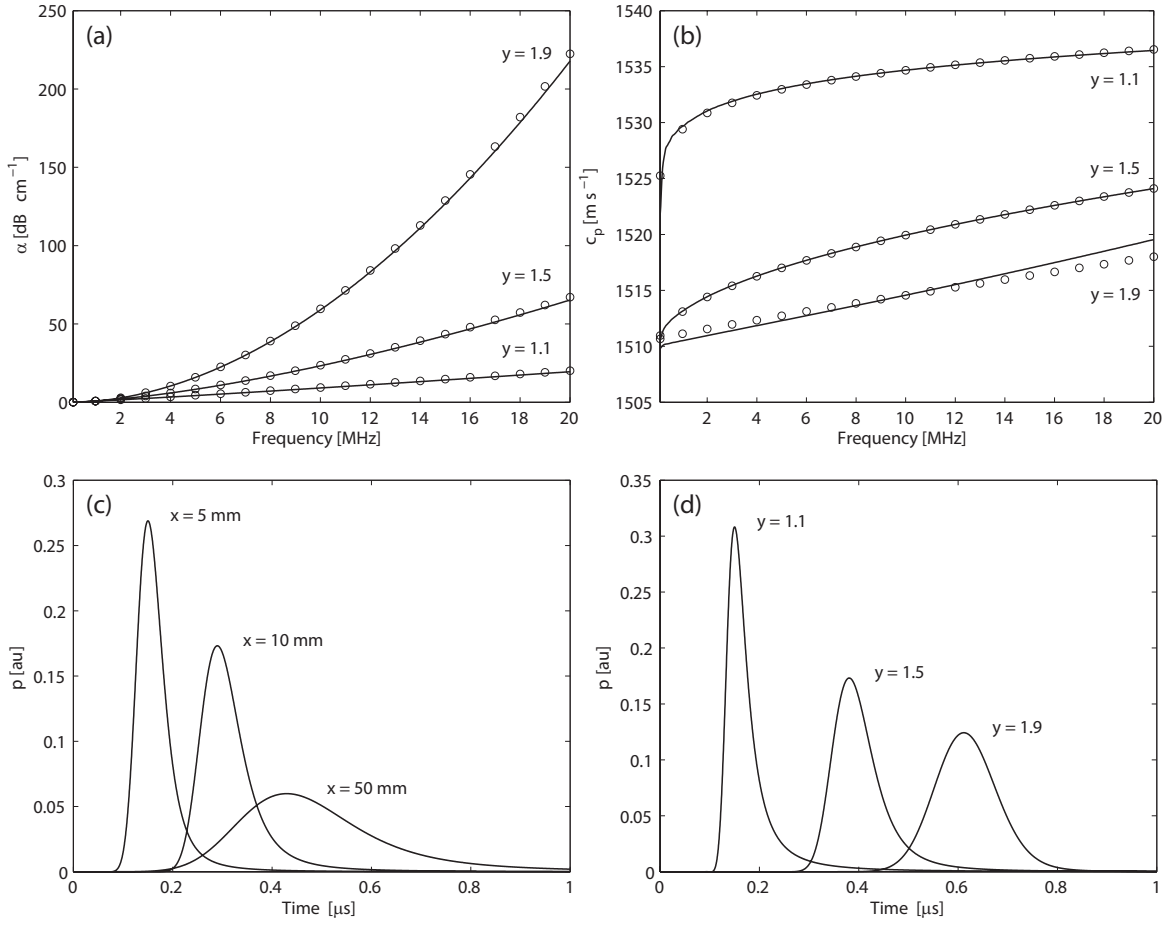

FIG. 2. Simulation of a monopolar plane wave pulse propagating through an absorbing medium with $\alpha_0=0.75$ dB MHz^{-y} cm^{-1} with $y=1.1$, 1.5, and 1.9. The values of (a) absorption, and (b) dispersion recovered from the simulation are shown as solid lines, with analytical values from 0.1 to 20 MHz shown as open circles. The change in the pulse shape with (c) distance x for a power law exponent of $y=1.5$, and (d) power law exponent y for a distance value of $x=10$ mm is also shown (the pulses have been translated in time for display).

based on a Kramers–Kronig dispersion relation in the form of Eq. (16) and thus the dispersive term in Eq. (28) breaks down as y approaches 1.

IV. NUMERICAL SIMULATION OF WAVE PROPAGATION THROUGH LOSSY MEDIA

A. Modeling wave propagation using coupled first-order equations

Equation (28) could be solved directly using standard numerical techniques, however, a more flexible framework is to divide the wave equation into its first-order constitutive components. For the lossless wave equation, the three standard coupled acoustic equations are the linearized equation of motion (Euler's inviscid force equation or conservation of momentum),

$$\frac{\partial \mathbf{u}}{\partial t} = -\frac{1}{\rho_0}\nabla p, \tag{29}$$

the linearized equation of continuity (conservation of mass),

$$\frac{\partial \rho}{\partial t} = -\rho_0 \nabla \cdot \mathbf{u}, \tag{30}$$

and the adiabatic equation of state,

$$p = c_0^2 \rho. \tag{31}$$

Here $\mathbf{u}$ is the acoustic velocity, and ρ and ρ_0 are the acoustic and ambient density, respectively. To model Eq. (28), the adiabatic equation of state is replaced with

$$p = c_0^2 \left\{ 1 + \tau \frac{\partial}{\partial t}(-\nabla^2)^{y/2-1} + \eta(-\nabla^2)^{(y+1)/2-1} \right\} \rho, \tag{32}$$

where the combination of Eqs. (29), (30), and (32) yields Eq. (28). The three bracketed terms account for the adiabatic equation of state, absorption, and dispersion, respectively.

For Fourier based pseudospectral and k-space models, the computational form of Eq. (32) is obtained by taking the spatial Fourier transform as defined in Eq. (5). This gives

$$p = c_0^2 \rho + \tau k^{y-2} \frac{\partial \rho}{\partial t} + \eta k^{y-1} \rho, \tag{33}$$

where $\partial\rho/\partial t$ is known from Eq. (30). This result highlights the advantage of the derived lossy operators; in the spatial frequency domain the fractional Laplacian becomes trivial to compute.

Modeling wave propagation using two coupled first-order equations (in which the equation of state is incorporated directly into the equation of continuity) has previously been considered in both finite-difference time-domain and

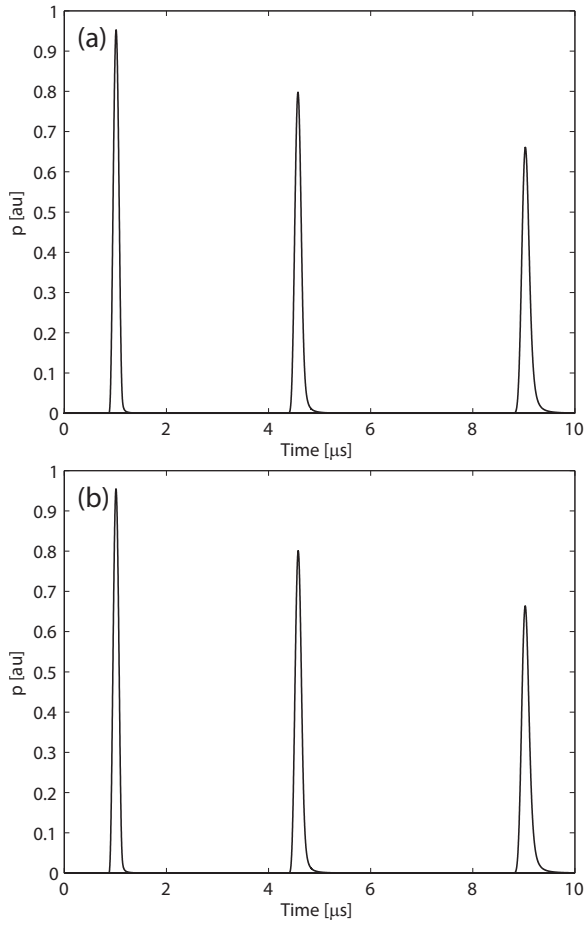

FIG. 3. Simulation of a monopolar pulse propagating through an absorbing medium with $\alpha_0=0.75$ dB MHz^{-y} cm^{-1} and $y=1.5$ for propagation distances of $x=1.32$, 6.75, and 13.5 mm (respectively) using (a) the material impulse response function, and (b) the fractional Laplacian equation of state developed here.

k-space models.[26,27] The separation of the pressure and velocity variables allows the inclusion of a perfectly matched layer (PML) near the edges of the computational domain.[33] This layer is assigned anisotropic absorption such that waves leaving the domain are absorbed and do not reappear on the opposite side as an artifact of the spatial derivative computation via the Fourier transform. Here this approach is extended to use three coupled first-order equations such that the equation of state is modeled explicitly.

B. Numerical simulations

To demonstrate the ability of the described equation of state to correctly model power law absorption and dispersion, the propagation of a broadband monopolar plane wave through a homogeneous absorbing medium was investigated. The computations were performed using the k-Wave MATLAB toolbox[34] which allows simulations of wave propagation in one, two, or three dimensions in homogeneous or heterogeneous media using a k-space pseudospectral method.[27,35,36] The simulations were performed in two-dimensions using a grid size of 32×4096 pixels (468.75 μm$\times$66 mm), a time step of 1 ns, and a total simulation time of 40 μs. The acoustic properties were based on human breast tissue, with a sound speed and density of 1510 m s^{-1} and 1020 kg m^{-3}, and an absorption coefficient α_0 of 1.3742×10^{-6} Np(rad/s)$^{-y}$ m^{-1} (equivalent to 0.75 dB MHz^{-y} cm^{-1}).[3] The initial pressure was defined as a single pixel line which was then smoothed using a frequency domain Hanning window.

Figures 2(a) and 2(b) illustrate the computed absorption and dispersion for power law exponents of 1.1, 1.5, and 1.9. These values were extracted from the time series recorded at two positions using the relations[37]

$$\alpha_{dB}=-\frac{20\log_{10}(A_2/A_1)}{100d}$$

$$c_p=-\frac{\omega d}{\phi_2-\phi_1}, \tag{34}$$

where α_{dB} is the absorption in units of dB cm^{-1}, $A_{1,2}$ and $\phi_{1,2}$ are the single-sided amplitude and phase spectrums, and d is the propagation distance in meters. To maximize the signal to noise, the values for 0–10 MHz were computed using the time-series recorded at 1 and 5 mm from the source, and the values for 10–20 MHz were computed using the time-series recorded at 1 and 2 mm. The simulated data are shown as a solid line, with analytical values from 0.1 to 20 MHz shown as open circles for comparison. The analytical values were computed using Eqs. (1) and (16), where ω_0 was chosen to be 10 MHz and the corresponding c_{ω_0} was extracted from the simulated data.

For the values of the power law exponent simulated, both the absorption and dispersion agree closely with the expected values. The deviation seen in the dispersion curve for a power law exponent of $y=1.9$ is due to numerical errors in computing $\partial\rho/\partial t$ via Eq. (30); the summation of this term with the remaining terms in Eq. (33) dependent on ρ rather than its derivative causes a small phase error. This is accentuated for $y=1.9$ due to the decreased signal to noise ratio [the absolute level absorption is significantly higher; see Fig. 2(a)], and the small amount of physical dispersion evident for this value of y.

Figure 2(c) illustrates the change in the pulse shape for a power law exponent of 1.5 (corresponding to breast tissue) and propagation distances of 5, 10, and 50 mm (the curves have been shifted temporally for display). As the wave propagates, the pulse is flattened and broadened as expected, and after 50 mm the magnitude is reduced to approximately 5% of its initial value. Figure 2(d) illustrates the change in pulse shape for a propagation distance of 10 mm and power law exponents of 1.1, 1.5, and 1.9. As the exponent is increased, the pulse is again flattened and broadened as the high frequencies are more readily absorbed. The amount of observable dispersion is also decreased; the pulse for $y=1.9$ looks almost symmetrical.

To further validate the simulation results, the pulse shapes calculated using the equation of state described here were compared to those computed using the material impulse response function (MIRF) defined by Szabo.[3,38] The comparison was computed using a smoothly varying sinusoidal monopolar excitation pulse with a pulse width of 125 ns (full

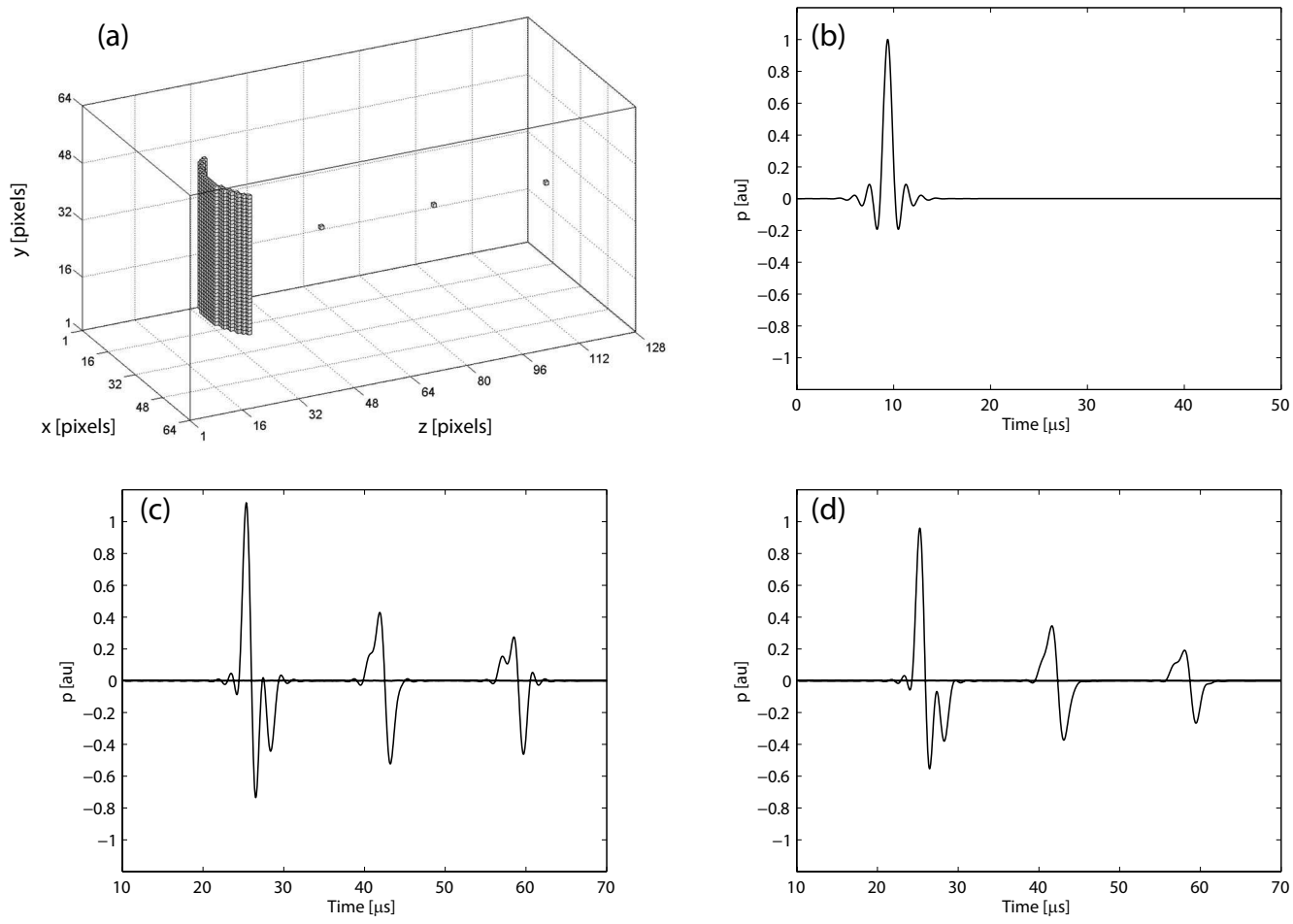

FIG. 4. Three-dimensional simulation of the wave-field from a curved linear array driven by a 50 ns square wave pulse filtered using a causal Kaiser filter. (a) Simulation schematic showing the transducer and the receiver positions. (b) Filtered input pulse. (c) Pulse shapes recorded at 2.5, 5, and 7.5 cm from the transducer surface with no absorption, and (d) with $\alpha_0=3$ dB MHz^{-y} cm^{-1} and $y=1.5$.

width at half maximum) and propagation distances of 1.32, 6.75, and 13.5 mm. The simulations were performed in one-dimension with a time step of 1 ns. The MIRF results [shown in Fig. 3(a)] were obtained by convolving the initial pressure with the MIRF, which itself was computed using the inverse fast Fourier transform of the material transfer function calculated using a maximum frequency of 50 MHz and a frequency step of 0.1 MHz.[3] The comparison [shown in Fig. 3(b)] was performed using a grid size of 1024 pixels (20 mm). The acoustic properties for both calculations were again set to those of human breast tissue, with a sound speed of 1510 m s^{-1}, and absorption parameters of $\alpha_0=0.75$ dB MHz^{-y} cm^{-1} and $y=1.5$. The two results show excellent agreement, confirming the ability of the derived equations to correctly model power absorption and dispersion. (The MIRF has also previously been compared with analytical Green's function solutions to Eq. (17).[12])

A final numerical example is shown in Fig. 4 to demonstrate the applicability of the developed model to 3D problems. This simulation was performed using a grid size of $64\times64\times128$ voxels ($5\times5\times10$ cm^3), a time step of 50 ns, and a total simulation time of 80 μs. The simulations were run on an NVIDIA Quadro FX 3700 graphics processing unit (GPU) with 512 Mbytes of memory using the k-Wave toolbox in conjunction with GPUmat.[34,39] The two simulations (with and without absorption) each took less than 3 min to complete. A curved linear array transducer was modeled using a cylinder segment 40 voxels in length (3.125 cm) with a curvature radius of 20 voxels (1.5625 cm) and an arc angle of 90° [see Fig. 4(a)]. This was driven by a 50 ns square wave pulse filtered using a causal Kaiser filter with a cutoff frequency of 0.65 MHz as shown in Fig. 4(b). The acoustic properties were again based on human breast tissue, with a sound speed of 1510 m s^{-1}, a density of 1020 kg m^{-3}, a power law exponent of 1.5, and an absorption coefficient of $\alpha_0=3$ dB MHz^{-y} cm^{-1} (due to the low frequency of the input, the latter was increased from its physiological value of 0.75 so the effects of absorption could easily be seen). Figures 4(c) and 4(d) show the shape of the wave pulse with and without absorption recorded at 2.5, 5, and 7.5 cm from the transducer surface along the midline.

V. SUMMARY

A new lossy equation of state that encapsulates power law absorption and dispersion is developed. This utilizes two lossy derivative operators based on the fractional Laplacian which perturb the adiabatic equation of state. The first, ini-

tially proposed by Chen and Holm,[14] is dependent on the fractional Laplacian of the temporal derivative of the density and accounts for power law attenuation. The second is dependent on the fractional Laplacian of the density and accounts for power law dispersion as required by the Kramers–Kronig relations. These operators can be efficiently incorporated into pseudospectral and *k*-space methods without the increase in memory required by their time-domain fractional counterparts. A framework for encoding the developed wave equation using three coupled first-order constitutive equations is discussed. The model is demonstrated to exhibit the required power law attenuation and dispersion through several one-, two-, and three-dimensional simulations.

ACKNOWLEDGMENTS

This work was supported by the Engineering and Physical Sciences Research Council, UK. The authors would like to acknowledge the insightful and thorough reports provided by the two anonymous reviewers.

[1]B. Fornberg, *A Practical Guide to Pseudospectral Methods* (Cambridge University Press, Cambridge, 1996).
[2]N. N. Bojarski, "The k-space formulation of the scattering problem in the time domain," J. Acoust. Soc. Am. **72**, 570–584 (1982).
[3]T. L. Szabo, *Diagnostic Ultrasound Imaging* (Elsevier, New York/Academic, London, 2004).
[4]G. ter Haar and C. Coussios, "High intensity focused ultrasound: Physical principles and devices," Int. J. Hyperthermia **23**, 89–104 (2007).
[5]*Photoacoustic Imaging and Spectroscopy*, edited by L. V. Wang (CRC, London, 2009).
[6]B. T. Cox and B. E. Treeby, "Artifact trapping during time reversal photoacoustic imaging for acoustically heterogeneous media," IEEE Trans. Med. Imaging **29**, 387–396 (2010).
[7]J. Laufer, B. Cox, E. Zhang, and P. Beard, "Quantitative determination of chromophore concentrations from 2D photoacoustic images using a nonlinear model-based inversion scheme," Appl. Opt. **49**, 1219–1233 (2010).
[8]J. J. Markham, R. T. Beyer, and R. B. Lindsay, "Absorption of sound in fluids," Rev. Mod. Phys. **23**, 353–411 (1951).
[9]T. L. Szabo, "Time domain wave equations for lossy media obeying a frequency power law," J. Acoust. Soc. Am. **96**, 491–500 (1994).
[10]W. Chen and S. Holm, "Modified Szabo's wave equation models for lossy media obeying frequency power law," J. Acoust. Soc. Am. **114**, 2570–2574 (2003).
[11]M. Liebler, S. Ginter, T. Dreyer, and R. E. Riedlinger, "Full wave modeling of therapeutic ultrasound: Efficient time-domain implementation of the frequency power-law attenuation," J. Acoust. Soc. Am. **116**, 2742–2750 (2004).
[12]J. F. Kelly, R. J. McGough, and M. M. Meerschaert, "Analytical time-domain Green's functions for power-law media," J. Acoust. Soc. Am. **124**, 2861–2872 (2008).
[13]M. J. Buckingham, "Theory of acoustic attenuation, dispersion, and pulse propagation in unconsolidated granular materials including marine sediments," J. Acoust. Soc. Am. **102**, 2579–2596 (1997).
[14]W. Chen and S. Holm, "Fractional Laplacian time-space models for linear and nonlinear lossy media exhibiting arbitrary frequency power-law dependency," J. Acoust. Soc. Am. **115**, 1424–1430 (2004).
[15]M. G. Wismer, "Finite element analysis of broadband acoustic pulses through inhomogenous media with power law attenuation," J. Acoust. Soc. Am. **120**, 3493–3502 (2006).
[16]M. Caputo, "Linear models of dissipation whose Q is almost frequency independent-II," Geophys. J. Int. **13**, 529–539 (1967).
[17]M. Ochmann and S. Makarov, "Representation of the absorption of nonlinear waves by fractional derivatives," J. Acoust. Soc. Am. **94**, 3392–3399 (1993).
[18]D. T. Blackstock, "Generalized Burgers equation for plane waves," J. Acoust. Soc. Am. **77**, 2050–2053 (1985).
[19]I. Podlubny, *Fractional Differential Equations* (Academic, New York, 1999).
[20]M. Moshrefi-Torbati and J. K. Hammond, "Physical and geometrical interpretation of fractional operators," J. Franklin Inst. **335**, 1077–1086 (1998).
[21]N. V. Sushilov and R. S. C. Cobbold, "Frequency-domain wave equation and its time-domain solutions in attenuating media," J. Acoust. Soc. Am. **115**, 1431–1436 (2004).
[22]A. I. Nachman, J. F. Smith III, and R. C. Waag, "An equation for acoustic propagation in inhomogeneous media with relaxation losses," J. Acoust. Soc. Am. **88**, 1584–1595 (1990).
[23]M. G. Wismer and R. Ludwig, "An explicit numerical time domain formulation to simulate pulsed pressure waves in viscous fluids exhibiting arbitrary frequency power law attenuation," IEEE Trans. Ultrason. Ferroelectr. Freq. Control **42**, 1040–1049 (1995).
[24]S. Ginter, "Numerical simulation of ultrasound-thermotherapy combining nonlinear wave propagation with broadband soft-tissue absorption," Ultrasonics **37**, 693–696 (2000).
[25]G. V. Norton and J. C. Novarini, "Including dispersion and attenuation directly in the time domain for wave propagation in isotropic media," J. Acoust. Soc. Am. **113**, 3024–3031 (2003).
[26]X. Yuan, D. Borup, J. Wiskin, M. Berggren, and S. A. Johnson, "Simulation of acoustic wave propagation in dispersive media with relaxation losses by using FDTD method with PML absorbing boundary condition," IEEE Trans. Ultrason. Ferroelectr. Freq. Control **46**, 14–23 (1999).
[27]M. Tabei, T. D. Mast, and R. C. Waag, "A k-space method for coupled first-order acoustic propagation equations," J. Acoust. Soc. Am. **111**, 53–63 (2002).
[28]J. C. Tillett, M. I. Daoud, J. C. Lacefield, and R. C. Waag, "A k-space method for acoustic propagation using coupled first-order equations in three dimensions," J. Acoust. Soc. Am. **126**, 1231–1244 (2009).
[29]M. I. Daoud and J. C. Lacefield, "Distributed three-dimensional simulation of B-mode ultrasound imaging using a first-order k-space method," Phys. Med. Biol. **54**, 5173 (2009).
[30]B. E. Treeby and B. T. Cox, "Fast, tissue-realistic models of photoacoustic wave propagation for homogeneous attenuating media," in *Photons Plus Ultrasound: Imaging and Sensing 2009* (SPIE, San Jose, CA, 2009), Vol. No. **7177**.
[31]K. R. Waters, M. S. Hughes, J. Mobley, G. H. Brandenburger, and J. G. Miller, "On the applicability of Kramers-Kronig relations for ultrasonic attenuation obeying a frequency power law," J. Acoust. Soc. Am. **108**, 556–563 (2000).
[32]K. R. Waters, J. Mobley, and J. G. Miller, "Causality-imposed (Kramers-Kronig) relationships between attenuation and dispersion," IEEE Trans. Ultrason. Ferroelectr. Freq. Control **52**, 822–823 (2005).
[33]J.-P. Berenger, "A perfectly matched layer for the absorption of electromagnetic waves," J. Comput. Phys. **114**, 185–200 (1994).
[34]B. E. Treeby and B. T. Cox, "k-Wave: MATLAB toolbox for the simulation and reconstruction of photoacoustic wave-fields," J. Biomed. Opt. **15**, 021314–1–12
[35]T. D. Mast, L. P. Souriau, D. L. D. Liu, M. Tabei, A. I. Nachman, and R. C. Waag, "A k-space method for large-scale models of wave propagation in tissue," IEEE Trans. Ultrason. Ferroelectr. Freq. Control **48**, 341–354 (2001).
[36]B. T. Cox, S. Kara, S. R. Arridge, and P. C. Beard, "k-space propagation models for acoustically heterogeneous media: Application to biomedical photoacoustics," J. Acoust. Soc. Am. **121**, 3453–3464 (2007).
[37]B. E. Treeby, B. T. Cox, E. Z. Zhang, S. K. Patch, and P. C. Beard, "Measurement of broadband temperature-dependent ultrasonic attenuation and dispersion using photoacoustics," IEEE Trans. Ultrason. Ferroelectr. Freq. Control **56**, 1666–1676 (2009).
[38]T. L. Szabo, "The material impulse response for broadband pulses in lossy media," Proc.-IEEE Ultrason. Symp. **1**, 748–751 (2003).
[39]GPUmat: GPU toolbox for MATLAB, http://www.gp-you.org (Last viewed 2/25/2010).